Supplementary information

Aqueous syntheses of anthracene-based mixed-ligand coordination polymers and their structural and optical properties

*Antti Marttinen, Manu Lahtinen**

Department of Chemistry, University of Jyväskylä, Jyväskylä, Finland.

Contents

NMR measurements

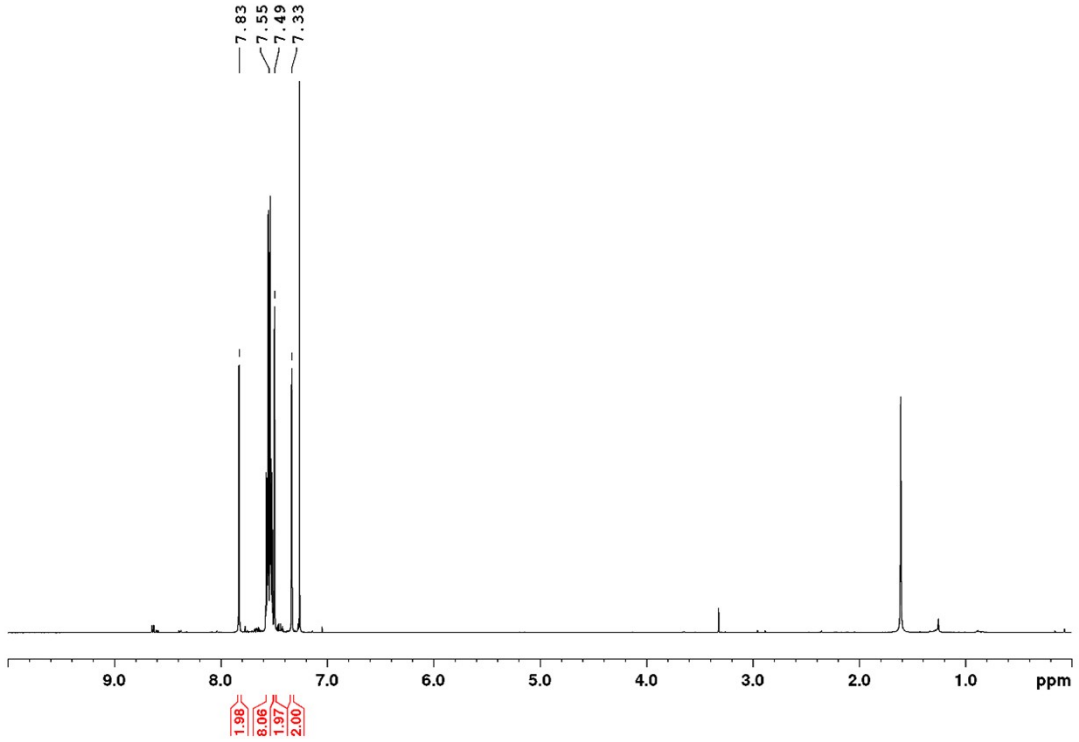

Figure S1. ^{1}H NMR spectrum of dia ligand in $CDCl_3$ (residual $CHCl_3$ peak at 7.26 ppm, impurity H_2O peak at 1.61 ppm)

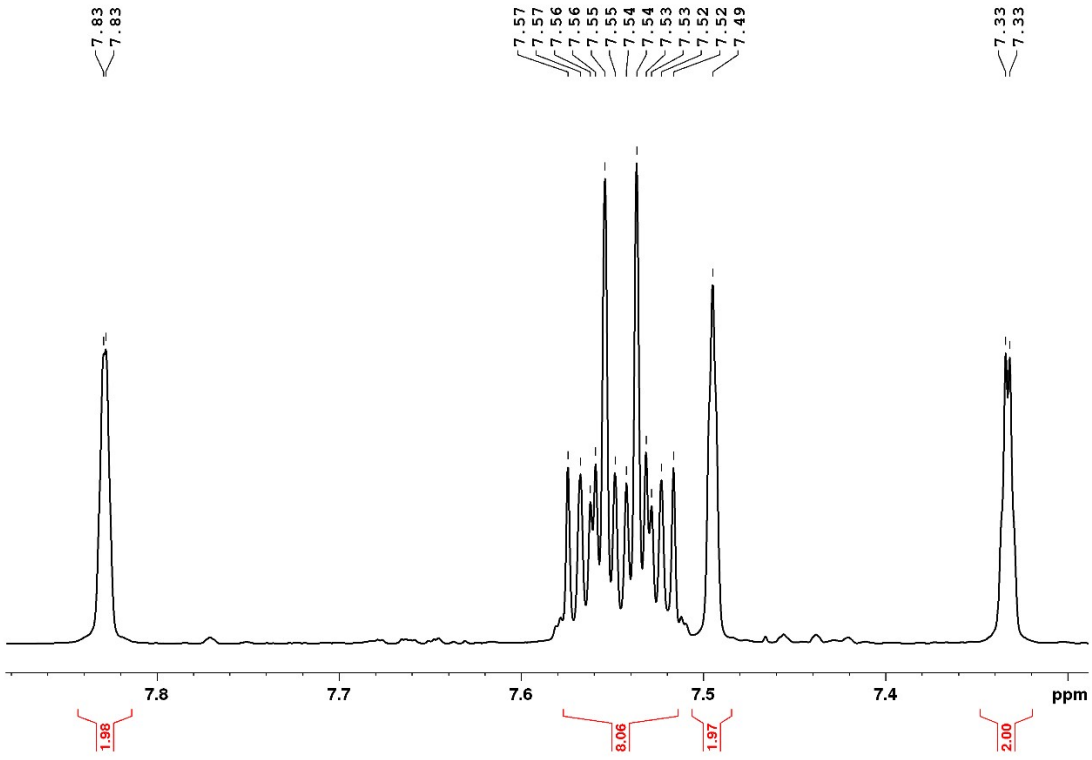

Figure S2. Zoomed aromatic region of ^{1}H NMR spectrum of dia ligand.

Characterization of $Na_2aip \cdot H_2O$ and $Na_2ata \cdot H_2O$

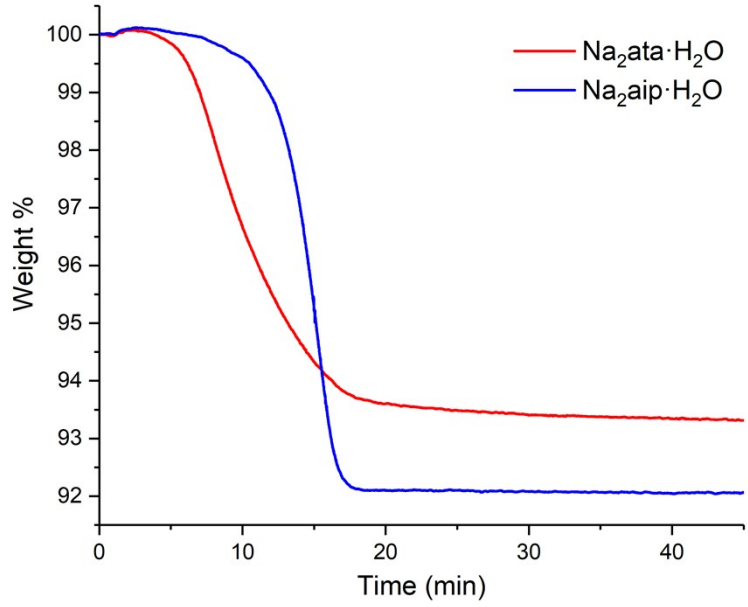

Figure S3. TGA curves of the synthesized $Na_2aip \cdot H_2O$ and $Na_2ata \cdot H_2O$ showing the evaporation of crystal water. Heated and held at 175 °C for 30 minutes.

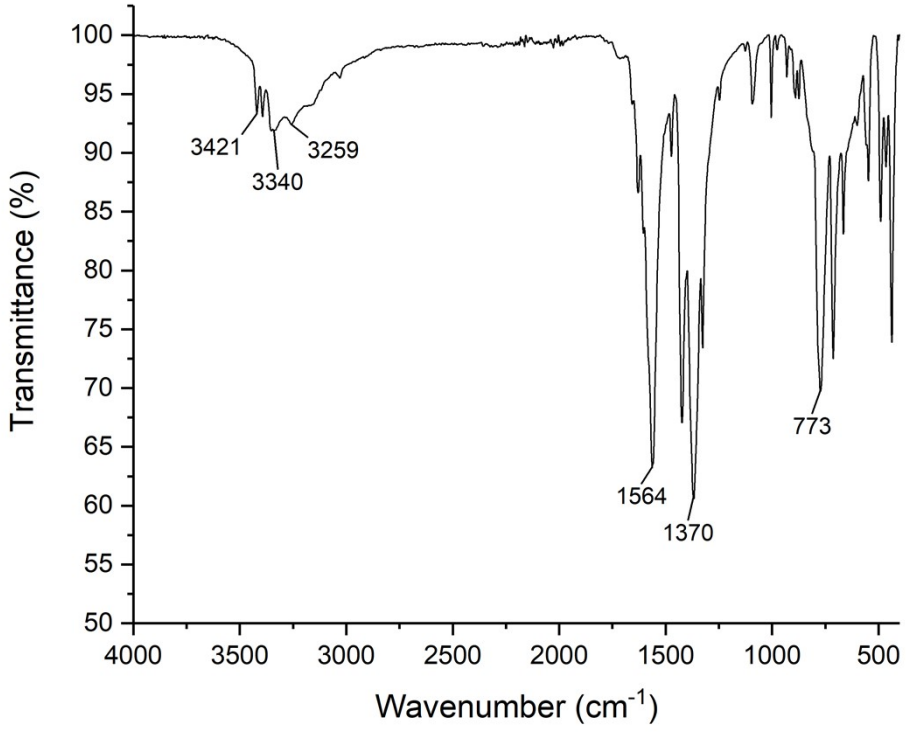

Figure S4. FT-IR spectra of $Na_2aip \cdot H_2O$.

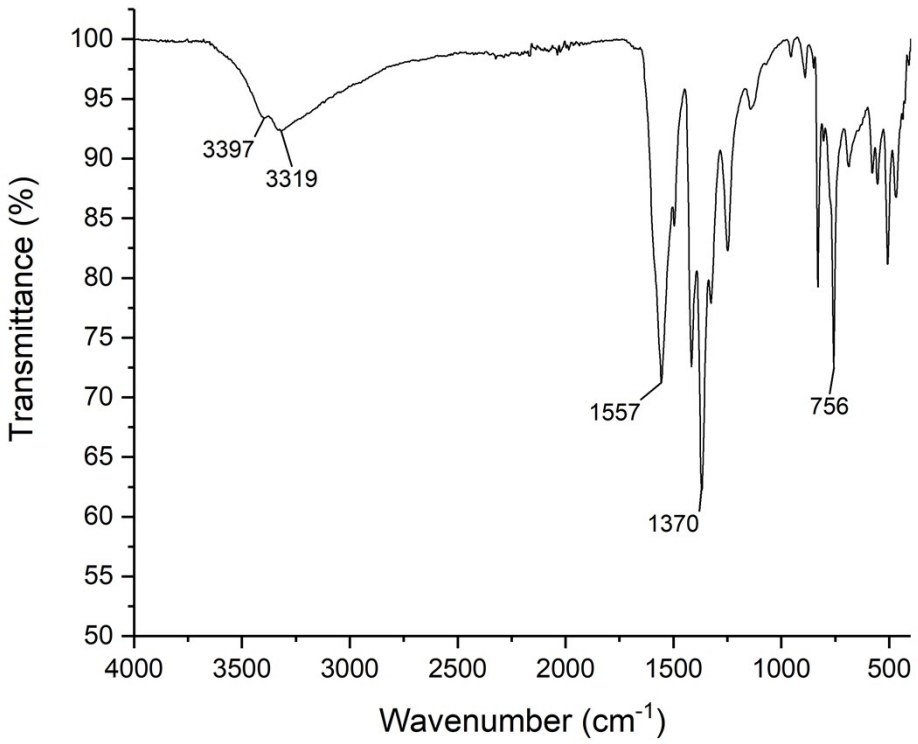

Figure S5. FT-IR spectra of $Na_2ata \cdot H_2O$.

Characterization of the new nitrate salt of dia ligand ($diaH_2(NO_3)_2$)

Single crystals of the nitrate salt of dia ligand were obtained by dissolving the powderous salt in hot methanol and leaving the solution to saturate in a closed glass vial. The salt crystallizes in the monoclinic space group of $P2_1/n$, showing one nitrate anion and half of dia ligand with a protonated imidazole moiety in the asymmetric unit. The imidazole hydrogen is strongly bonded to the nitrate oxygen with a bond length of 1.818(1) Å (Fig. S6A). Dia molecules pack in the crystal lattice so that they alternate between a horizontal and a vertical orientation at a roughly 90-degree angle relative to each other. This creates an angular zigzag structure (Fig. S6B). The nitrate anions occupy the empty spaces in the structure next to the anthracene rings of the neighboring ligands (Fig. S6C).

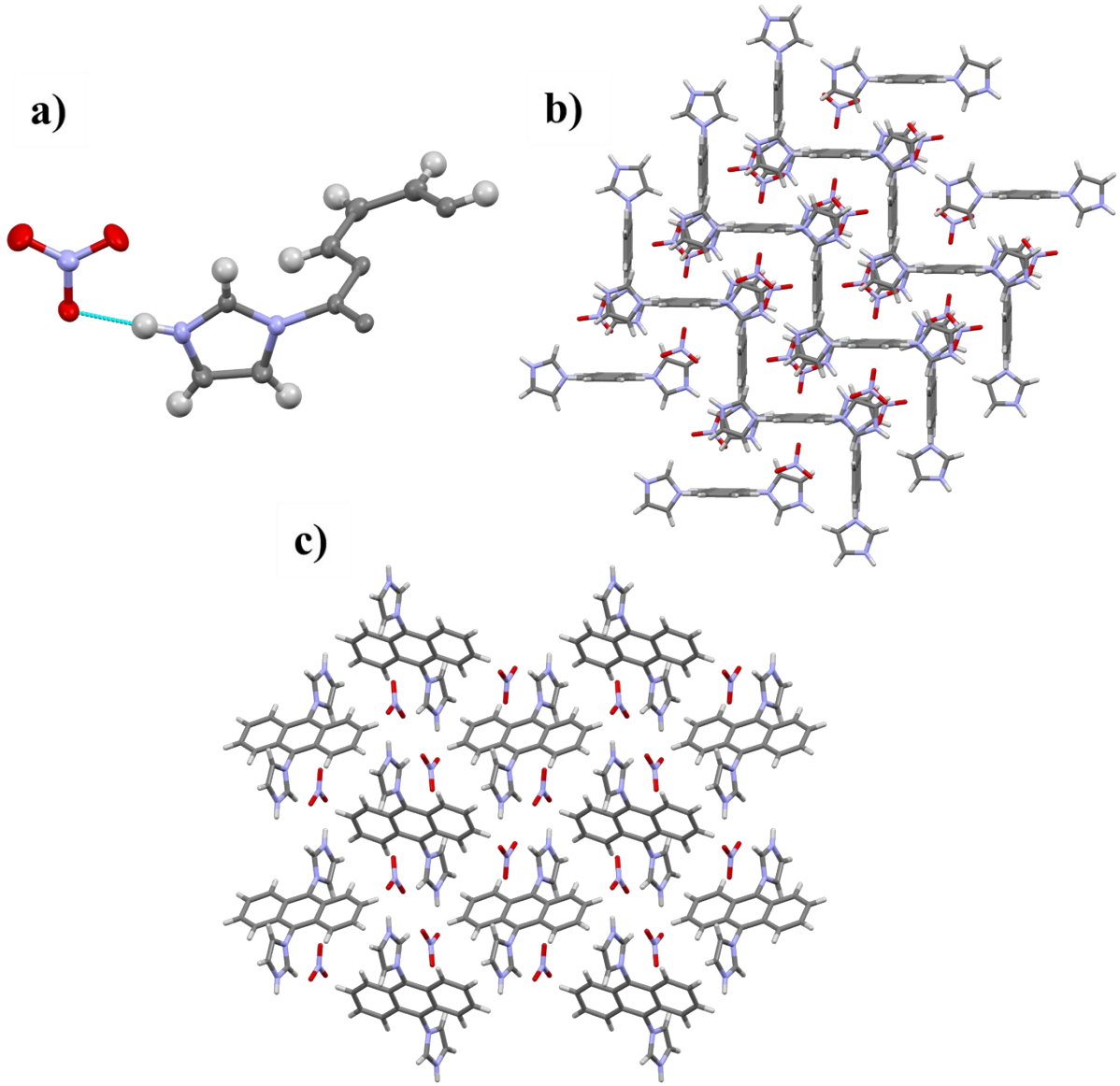

Figure S6. Asymmetric unit of dia$H_2(NO_3)_2$, hydrogen bonding represented as a blue line. Thermal ellipsoids of atoms are presented at 50 % probability level. b) zigzag packing of dia molecules, and c) crystal structure of dia$H_2(NO_3)_2$ viewed along the *a*-axis.

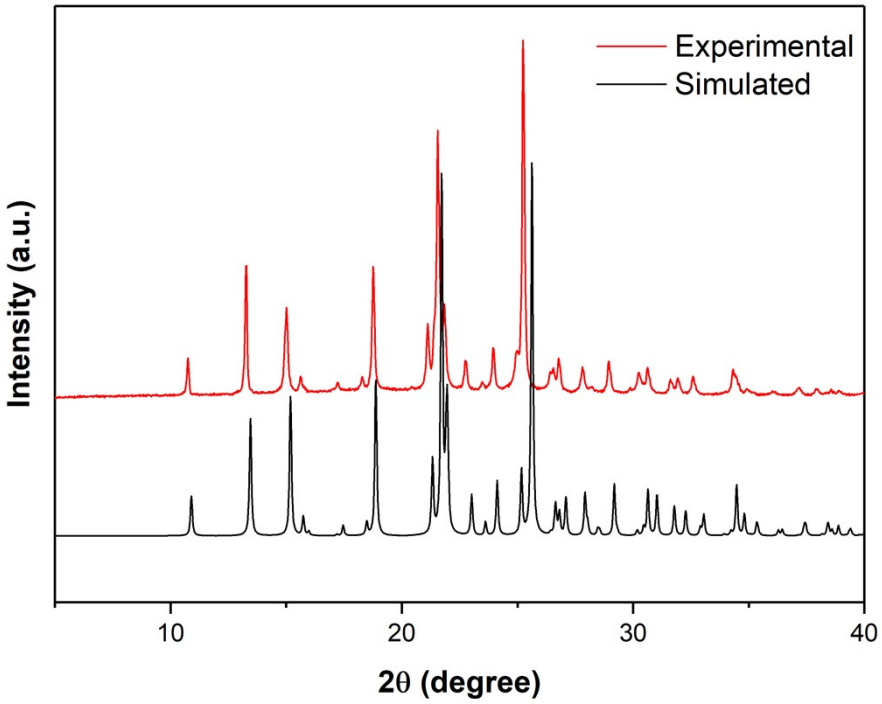

Figure S7. PXRD pattern comparison of the synthesized dia$H_2(NO_3)_2$ bulk powder and the simulated pattern from the SCXRD data.

Table S1: Crystallographic data of dia$H_2(NO_3)_2$ salt.

CCDC deposition number	2309443
Empirical formula	$C_{20}H_{16}N_6O_6$
Formula weight	436.39
Temperature/K	120.01(10)
Crystal system	monoclinic
Space group	$P2_1/n$
a/Å	7.17230(10)
b/Å	10.30090(10)
c/Å	13.34380(10)
α/°	90
β/°	99.6960(10)
γ/°	90
Volume/Å^3	971.773(18)
Z	2
ρ_{calc}g/cm^3	1.491
μ/mm^{-1}	0.961
F(000)	452.0
Crystal size/mm^3	0.141 × 0.118 × 0.098
2Θ range for data collection/°	10.91 to 158.142
Reflections collected	10532
Independent reflections	2060 [R_{int} = 0.0232, R_{sigma} = 0.0183]
Data/restraints/parameters	2060/0/145
Goodness-of-fit on F^2	1.098
Final R indexes [I>=2σ (I)]	R_1 = 0.0377, wR_2 = 0.1011
Final R indexes [all data]	R_1 = 0.0406, wR_2 = 0.1034
Largest diff. peak/hole / e Å^{-3}	0.19/-0.29

Crystallographic data of the MOF/CP single crystals

Table S2: Crystallographic data of the crystallized compounds **1-6** and **6B** (-153 °C and 0 °C)

Structure	**1**	**2**	**3**
CCDC deposition number	2309435	2309436	2309437
Empirical formula	$C_{56}H_{50}Cu_2N_{10}O_{14}$	$C_{56}H_{48}N_{10}Ni_2O_{13}$	$C_{56}H_{44}Cu_2N_{10}O_{12}$
Formula weight	1214.14	1186.46	1176.09
Temperature/K	120.00(10)	120.01(10)	120.01(10)
Crystal system	monoclinic	monoclinic	triclinic
Space group	$P2_1/n$	$P2_1/n$	P-1
a/Å	10.15270(10)	10.1841(2)	10.8808(3)
b/Å	21.4379(3)	22.1378(4)	11.1603(3)
c/Å	12.6218(2)	12.2623(2)	12.5136(3)
α/°	90	90	111.044(2)
β/°	96.0470(10)	96.771(2)	107.145(2)
γ/°	90	90	95.432(2)
Volume/Å^3	2731.88(6)	2745.30(9)	1320.49(6)
Z	2	2	1
ρ_{calc}g/cm^3	1.476	1.435	1.479
μ/mm^{-1}	1.610	1.477	1.619
F(000)	1252.0	1228.0	604.0
Crystal size/mm^3	0.221 × 0.042 × 0.035	0.12 × 0.021 × 0.01	0.092 × 0.077 × 0.052
2Θ range for data collection/°	8.162 to 154.836	7.988 to 153.11	8.094 to 159.038
Reflections collected	16926	30247	21942
Independent reflections	5631 [R_{int} = 0.0317, R_{sigma} = 0.0319]	5747 [R_{int} = 0.0848, R_{sigma} = 0.0517]	5597 [R_{int} = 0.0352, R_{sigma} = 0.0314]
Data/restraints/parameters	5631/0/385	5747/8/399	5597/1/389
Goodness-of-fit on F^2	1.042	1.082	1.078
Final R indexes [I>=2σ (I)]	R_1 = 0.0396, wR_2 = 0.1010	R_1 = 0.0572, wR_2 = 0.1235	R_1 = 0.0476, wR_2 = 0.1154
Final R indexes [all data]	R_1 = 0.0458, wR_2 = 0.1059	R_1 = 0.0891, wR_2 = 0.1377	R_1 = 0.0560, wR_2 = 0.1198
Largest diff. peak/hole / e Å^{-3}	0.75/-0.56	0.51/-0.61	0.52/-0.50

Table S2: Continues

Structure	**4**	**5**	**6**
CCDC deposition number	2309438	2309439	2309440
Empirical formula	$C_{76}H_{55}N_{14}Ni_2O_{10.5}$	$C_{72}H_{44}Cu_8N_8O_{32}S_4$	$C_{134}H_{146}N_{26}Ni_3O_{34}S_2$
Formula weight	1449.76	2169.71	2905.01
Temperature/K	120.01(10)	120.15	120.15
Crystal system	triclinic	triclinic	monoclinic
Space group	*P*-1	*P*-1	$P2_1/n$
a/Å	11.2569(11)	10.1534(2)	13.63110(10)
b/Å	13.4025(17)	10.8388(2)	30.64140(10)
c/Å	13.5086(13)	17.2424(2)	16.96660(10)
α/°	61.328(11)	88.5480(10)	90
β/°	71.172(9)	89.922(2)	104.0130(10)
γ/°	75.382(10)	84.669(2)	90
Volume/Å^3	1680.8(4)	1888.72(6)	6875.65(7)
Z	1	1	2
ρ_{calc}g/cm^3	1.432	1.908	1.403
μ/mm^{-1}	1.309	4.302	1.489
F(000)	749.0	1084.0	3040.0
Crystal size/mm^3	0.101 × 0.02 × 0.016	0.043 × 0.024 × 0.019	0.151 × 0.111 × 0.081
2Θ range for data collection/°	7.57 to 147.988	5.126 to 159.054	5.768 to 158.152
Reflections collected	24885	34793	75492
Independent reflections	6775 [R_{int} = 0.0842, R_{sigma} = 0.0686]	8038 [R_{int} = 0.0412, R_{sigma} = 0.0309]	14648 [R_{int} = 0.0264, R_{sigma}a = 0.0203]
Data/restraints/parameters	6775/0/487	8038/39/556	14648/0/935
Goodness-of-fit on F^2	1.078	1.031	1.063
Final R indexes [I>=2σ (I)]	R_1 = 0.0644, wR_2 = 0.1346	R_1 = 0.0438, wR_2 = 0.1075	R_1 = 0.0506, wR_2 = 0.1334
Final R indexes [all data]	R_1 = 0.0989, wR_2 = 0.1493	R_1 = 0.0526, wR_2 = 0.1118	R_1 = 0.0546, wR_2 = 0.1366
Largest diff. peak/hole / e Å^{-3}	0.87/-0.48	1.04/-0.91	1.15/-0.82

Table S2: Continues

Structure	**6B (-153 °C)**	**6B (0 °C)**
CCDC deposition number	2309441	2309442
Empirical formula	$C_{128}H_{136}N_{24}Ni_3O_{34}S_2$	$C_{128}H_{132}N_{24}Ni_3O_{32}S_2$
Formula weight	2794.85	2758.82
Temperature/K	120.00(10)	273.00(10)
Crystal system	monoclinic	monoclinic
Space group	$P2_1/n$	$P2_1/n$
a/Å	13.61780(10)	13.5935(3)
b/Å	29.7718(2)	29.6842(9)
c/Å	17.1157(2)	17.6639(5)
α/°	90	90
β/°	104.0980(10)	104.823(3)
γ/°	90	90
Volume/Å^3	6730.15(11)	6890.4(3)
Z	2	2
ρ_{calc}g/cm^3	1.379	1.330
μ/mm^{-1}	1.495	1.442
F(000)	2920.0	2880.0
Crystal size/mm^3	0.178 × 0.123 × 0.108	0.128 × 0.072 × 0.055
2Θ range for data collection/°	5.938 to 158.146	5.954 to 158.89
Reflections collected	73390	74695
Independent reflections	14350 [R_{int} = 0.0298, R_{sigma} = 0.0218]	14655 [R_{int} = 0.0753, R_{sigma} = 0.0404]
Data/restraints/parameters	14350/55/623	14655/7/689
Goodness-of-fit on F^2	1.083	1.053
Final R indexes [I>=2σ (I)]	R_1 = 0.0857, wR_2 = 0.2222	R_1 = 0.0809, wR_2 = 0.2226
Final R indexes [all data]	R_1 = 0.0911, wR_2 = 0.2267	R_1 = 0.0943, wR_2 = 0.2324
Largest diff. peak/hole / e Å^{-3}	1.72/-1.57	1.36/-1.28

Table S3: Selected bond lengths (Å) and angles (°) for structure **1**

Cu1-O13	1.9744(14)	Cu1-N26	1.9801(18)
Cu1-O24#1	2.0173(14)	Cu1-N1	1.9815(18)
Cu1-O25#1	2.7128(17)	Cu1-N22#2	2.2999(18)
O13-Cu1-O24#1	155.40(6)	O13-Cu1-N26	91.08(7)
O13-Cu1-O25#1	101.78(6)	O13-Cu1-N1	87.91(7)
O24#1-Cu1-O25#1	53.62(5)	O13-Cu1-N22#2	107.59(7)
O24#1-Cu1-N22#2	97.00(6)	N26-Cu1-N1	174.30(8)

Symmetry codes: #1 1+X,+Y,+Z; #2 1/2+X,1/2-Y,1/2+Z;

Table S4: Selected bond lengths (Å) and angles (°) for structure **2**

Ni1-O13	2.008(2)	Ni1-N26	2.052(3)
Ni1-O24#1	2.078(2)	Ni1-N1	2.040(3)
Ni1-O25#1	2.278(2)	Ni1-N22#2	2.113(3)
O13-Ni1-O24#1	162.97(9)	O13-Ni1-N26	90.55(10)
O13-Ni1-O25#1	102.48(9)	O13-Ni1-N1	88.16(10)
O24#1-Ni1-O25#1	60.50(8)	O13-Ni1-N22#2	101.34(10)
O24#1-Ni1-N22#2	95.65(10)	N1-Ni1-N26	175.69(11)

Symmetry codes: #1 -1+X,+Y,+Z; #2 -1/2+X,1/2-Y,-1/2+Z

Table S5: Selected bond lengths (Å) and angles (°) for structure **3**

Cu1-O1	1.9607(15)	Cu2-O32	1.9514(17)
Cu1-O1#1	1.9607(15)	Cu2-O32#2	1.9513(17)
Cu1-N8#1	1.9923(19)	Cu2-N30#2	2.0153(19)
Cu1-O2	2.6044(19)	Cu2-O40	2.535(2)
Cu1-N8	1.9922(19)	Cu2-N30	2.0153(19)
O1-Cu1-N8#1	89.64(7)	O32-Cu2-N30	91.19(8)
O1-Cu1-N8	90.36(7)	O32-Cu2-N30#2	88.81(8)
O2-Cu1-N8	91.34(8)	O40-Cu2-O32	89.29(8)
O2-Cu1-N8#1	88.66(8)	O40-Cu2-N30	85.20(8)

Symmetry codes: #1 1-X,-Y,-Z; #2 3-X,2-Y,1-Z

Table S6: Selected bond lengths (Å) and angles (°) for structure **4**

Ni1-O1	2.058(2)	Ni2-O32	2.029(2)
Ni1-N8	2.084(3)	Ni2-O51	2.105(3)
Ni1-N20	2.111(3)	Ni2-N39	2.055(3)
O1-Ni1-N8	86.97(10)	O32-Ni2-O51#2	87.29(10)
O1-Ni1-N8#1	93.04(10)	O32-Ni2-O51	92.71(10)
O1-Ni1-N20#1	84.93(10)	O32-Ni2-N39	91.80(11)
O1-Ni1-N20	95.07(10)	O32-Ni2-N39#2	88.20(11)
N8-Ni1-N20	85.19(11)	N39-Ni2-O51#2	90.79(11)
N8-Ni1-N20#1	94.81(11)	N39-Ni2-O51	89.21(11)

Symmetry codes: #1 2-X,1-Y,-Z; #2 1-X,2-Y,-Z

Table S7: Selected bond lengths (Å) and angles (°) for structure **5**

Cu1-N1	1.985(3)	Cu3-O26	2.295(3)
Cu1-O13	1.950(2)	Cu3-N30	2.003(3)
Cu1-O14	1.951(2)	Cu3-O42	1.968(2)
Cu1-O28#3	1.967(2)	Cu3-O43	1.931(2)
Cu1-O53A#4	2.325(3)	Cu3-O57#3	1.931(2)
Cu2-O13	2.007(2)	Cu4-O24#2	2.392(2)
Cu2-O13#5	1.994(2)	Cu4-O42#1	1.983(2)
Cu2-O29#6	1.942(2)	Cu4-O42#2	2.003(2)
Cu2-O15	1.940(2)	Cu4-O45#1	1.935(2)
Cu2-O54A#4	2.345(3)	Cu4-O58	1.940(2)
O13-Cu1-N1	171.95(11)	O42-Cu3-N30	173.32(12)
O14-Cu1-O28#3	154.68(12)	O43-Cu3-O57#3	155.72(12)
O15-Cu2-O13#5	176.67(10)	O58-Cu4-O42#1	175.89(10)
O29#6-Cu2-O13	164.28(10)	O45#1-Cu4-O42#2	164.25(10)

Symmetry codes: #1 1-X,2-Y,2-Z; #2 +X,1+Y,+Z; #3 +X,-1+Y,+Z; #4 -1+X,-1+Y,+Z; #5 -X,-Y,1-Z; #6 -X,1-Y,1-Z

Table S8: Selected bond lengths (Å) and angles (°) for structure **6**

Ni1-O72#1	2.1284(14)	Ni2-O61	2.0578(14)
Ni1-N1	2.0909(17)	Ni2-O76#3	2.0616(15)
Ni1-N13	2.0784(17)	Ni2-O77	2.0806(14)
N1#2-Ni1-O72#1	86.81(6)	Ni2-N34	2.0789(17)
N1-Ni1-O72#1	93.19(6)	Ni2-N37	2.0955(17)
N13-Ni1-O72#1	90.65(6)	Ni2-N58#4	2.0968(18)
N13#2-Ni1-O72#1	89.35(6)	O61-Ni2-O77	88.44(6)
N13-Ni1-N1#2	86.96(7)	O61-Ni2-N34	85.63(6)
N13-Ni1-N1	93.05(7)	O61-Ni2-N58#4	99.18(7)
O61-Ni2-O76#3	175.31(6)	N34-Ni2-O77	173.47(6)

Symmetry codes: #1 +X,+Y,1+Z; #2 1-X,1-Y,2-Z; #3 1/2+X,3/2-Y,1/2+Z; #4 1+X,+Y,+Z;

Table S9: Selected bond lengths (Å) and angles (°) for structure **6B (-153 °C)**

Ni1-O72#1	2.100(3)	Ni2-O75#4	2.024(2)
Ni1-N1	2.090(3)	Ni2-O77	2.102(3)
Ni1-N13	2.089(3)	Ni2-O61	2.029(3)
N1#3-Ni1-O72#2	85.14(11)	Ni2-N58#5	2.096(3)
N1-Ni1-O72#2	94.86(11)	Ni2-N34	2.099(3)
N13-Ni1-O72#1	90.78(11)	Ni2-N37	2.077(3)
N13#3-Ni1-O72#1	89.21(11)	O61-Ni2-O77	90.76(11)
N13-Ni1-N1#3	93.08(10)	O61-Ni2-N58#5	88.65(15)
N13-Ni1-N1	86.92(10)	O61-Ni2-N34	93.97(11)
O75#4-Ni2-O61	178.54(12)	N34-Ni2-O77	175.18(11)

Symmetry codes: #1 1/2+X,1/2-Y,-1/2+Z; #2 3/2-X,1/2+Y,1/2-Z; #3 2-X,1-Y,-Z; #4 1/2+X,1/2-Y,1/2+Z; #5 1+X,+Y,+Z

Table S10: Selected bond lengths (Å) and angles (°) for structure **6B (0 °C)**

Ni1-O71#1	2.112(3)	Ni2-O76#4	2.054(2)
Ni1-N1	2.097(3)	Ni2-O77	2.108(3)
Ni1-N13	2.087(3)	Ni2-O61	2.037(2)
N1#3-Ni1-O71#2	86.11(11)	Ni2-N58#5	2.103(3)
N1-Ni1-O71#2	93.89(11)	Ni2-N34	2.101(3)
N13-Ni1-O71#1	90.36(11)	Ni2-N37	2.077(3)
N13#3-Ni1-O71#1	89.64(11)	O61-Ni2-O77	89.17(10)
N13-Ni1-N1#3	87.54(11)	O61-Ni2-N58#5	89.83(12)
N13-Ni1-N1	92.45(11)	O61-Ni2-N34	86.97(11)
O61-Ni2-O76#4	178.96(11)	N34-Ni2-O77	175.99(11)

Symmetry codes: #1 1-X,1-Y,1-Z; #2 +X,+Y,-1+Z; #3 1-X,1-Y,-Z; #4 -1/2+X,1/2-Y,-1/2+Z; #5 1+X,+Y,+Z;

Table S11: Hydrogen bond table of structure **1**

D	H	A	d(D-H)/Å	d(H-A)/Å	d(D-A)/Å	D-H-A/°
O38	H38A	O39	0.85	1.94	2.784(3)	173.8
O38	H38B	O24	0.85	1.98	2.787(2)	157.0
N22	H22B	O38#1	0.99	2.05	2.968(3)	153.7
O40B	H40A	O15	0.85	1.95	2.785(11)	166.5
O39	H39A	O40A	0.85	2.19	2.992(8)	156.3
O39	H39B	O25#2	0.85	1.98	2.825(3)	170.4
O40A	H40C	O15	0.85	1.93	2.625(11)	138.6

Symmetry codes: #1 1/2+X,1/2-Y,-1/2+Z; #2 1/2+X,1/2-Y,1/2+Z

Table S12: Hydrogen bond table of structure **2**

D	H	A	d(D-H)/Å	d(H-A)/Å	d(D-A)/Å	D-H-A/°
O39	H39A	O24#1	0.87	1.86	2.711(3)	163.9
O39	H39B	O38B	0.87	2.03	2.877(10)	163.3
O39	H39B	O38A	0.87	1.94	2.796(5)	169.6
O38A	H38C	O25	0.87	2.02	2.887(5)	177.2
O38A	H38D	O15#1	0.87	2.11	2.977(6)	172.3
O40A	H40A	O40A#2	0.87	2.39	2.99(2)	127.0

Symmetry codes: #1 1/2+X,1/2-Y,1/2+Z; #2 2-X,-Y,2-Z

Table S13: Hydrogen bond table of structure **3**

D	H	A	d(D-H)/Å	d(H-A)/Å	d(D-A)/Å	D-H-A/°
O40	H40A	O33#1	0.87	1.90	2.716(3)	154.8
O40	H40B	O2#2	0.87	2.00	2.851(3)	164.7
O39	H39A	O1#3	0.87	2.01	2.873(3)	168.7
O39	H39B	O40	0.87	2.02	2.877(3)	168.5
N6	H6B	O2	0.89	1.94	2.636(5)	134.3

Symmetry codes: #1 3-X,2-Y,1-Z; #2 2-X,1-Y,1-Z; #3 1+X,1+Y,1+Z

Table S14: Hydrogen bond table of structure **4**

D	H	A	d(D-H)/Å	d(H-A)/Å	d(D-A)/Å	D-H-A/°
O51	H51A	O33	0.87	1.86	2.641(4)	148.7
O51	H51B	O2	0.87	1.95	2.785(3)	158.7
N7	H7A	O1#1	0.89	1.92	2.645(7)	137.7
N7	H7B	O33	0.89	2.32	2.898(7)	122.6
N38	H38A	O33#2	0.89	1.93	2.636(9)	134.7

Symmetry codes: #1 1-X,1-Y,-Z; #2 -X,2-Y,-Z

Table S15: Hydrogen bond table of structure **5**

D	H	A	d(D-H)/Å	d(H-A)/Å	d(D-A)/Å	D-H-A/°
O13	H13	O55A#1	1.00	1.91	2.781(3)	143.7
O13	H13	O55B#1	1.00	1.87	2.71(2)	139.2
O42	H42	O25#2	1.00	1.89	2.772(3)	145.2
C34	H34	O26	0.95	2.37	2.969(4)	120.7

Symmetry codes: #1 1-X,1-Y,1-Z; #2 1-X,1-Y,2-Z

Table S16: Hydrogen bond table of structure **6**

D	H	A	d(D-H)/Å	d(H-A)/Å	d(D-A)/Å	D-H-A/°
O77	H77A	O62	0.85	1.95	2.675(2)	142.7
O77	H77B	O75#1	0.85	1.94	2.698(2)	147.8
O94	H94A	O97	0.85	1.94	2.709(3)	150.5
O94	H94B	O75	0.85	2.07	2.863(2)	155.5
O95	H95A	O94	0.85	1.97	2.807(3)	168.3
O95	H95B	O62#2	0.85	2.08	2.905(2)	164.3
O96	H96A	O95	0.85	1.97	2.801(3)	165.4
O97	H97A	O96	0.85	1.92	2.765(4)	173.6
O97	H97B	O98A	0.85	1.98	2.751(5)	149.6
O83	H83A	O82	0.85	1.90	2.735(5)	168.4
O83	H83B	O82#3	0.85	2.19	2.998(5)	160.0

Symmetry codes: #1 1/2+X,3/2-Y,1/2+Z; #2 -1/2+X,3/2-Y,-1/2+Z; #3 1-X,1-Y,1-Z

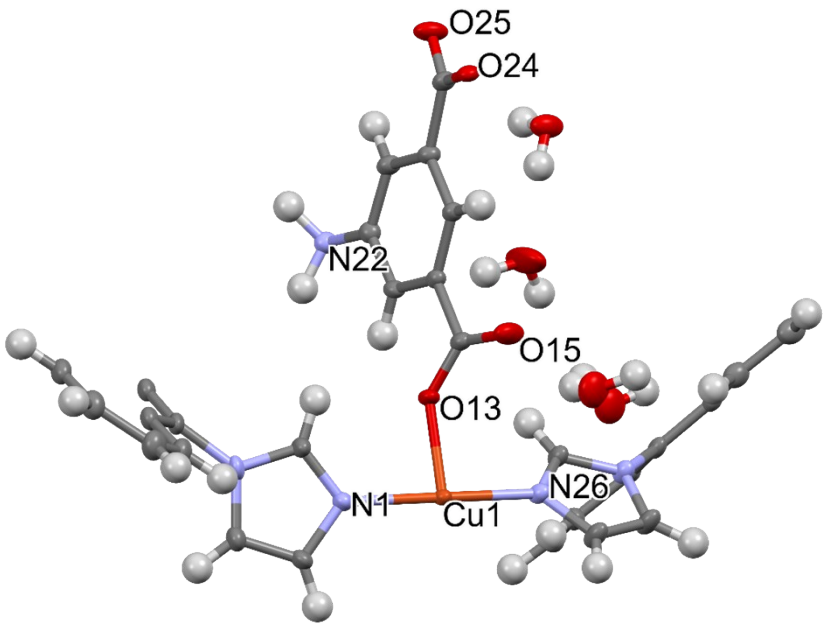

Figure S8. Asymmetric unit of structure **1**. Thermal ellipsoids of atoms are presented at 50 % probability level.

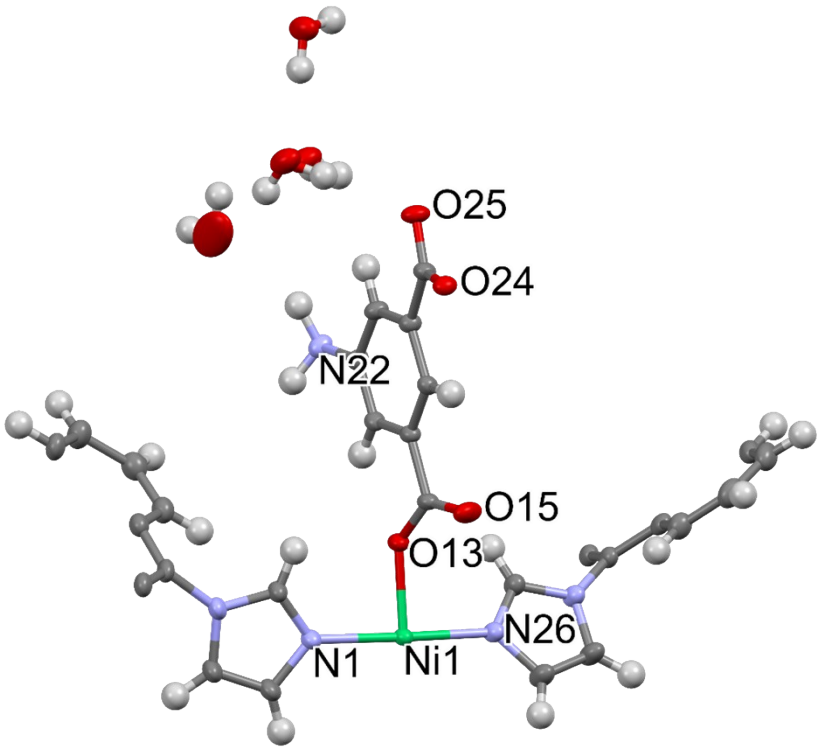

Figure S9. Asymmetric unit of structure **2.** Thermal ellipsoids of atoms are presented at 50 % probability level. The enlarged water molecule is disordered with partial occupancy of 0.5 but possibly due to its volatile nature the other half could not be found from the electron density maps.

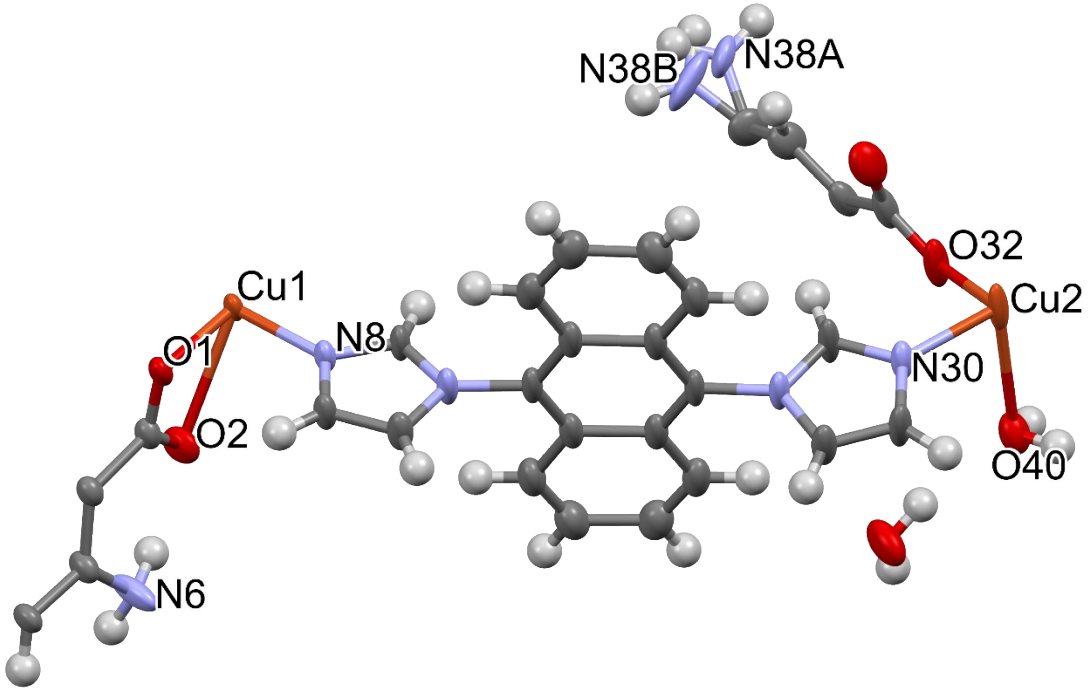

Figure S10. Asymmetric unit of structure **3.** Thermal ellipsoids of atoms are presented at 50 % probability level.

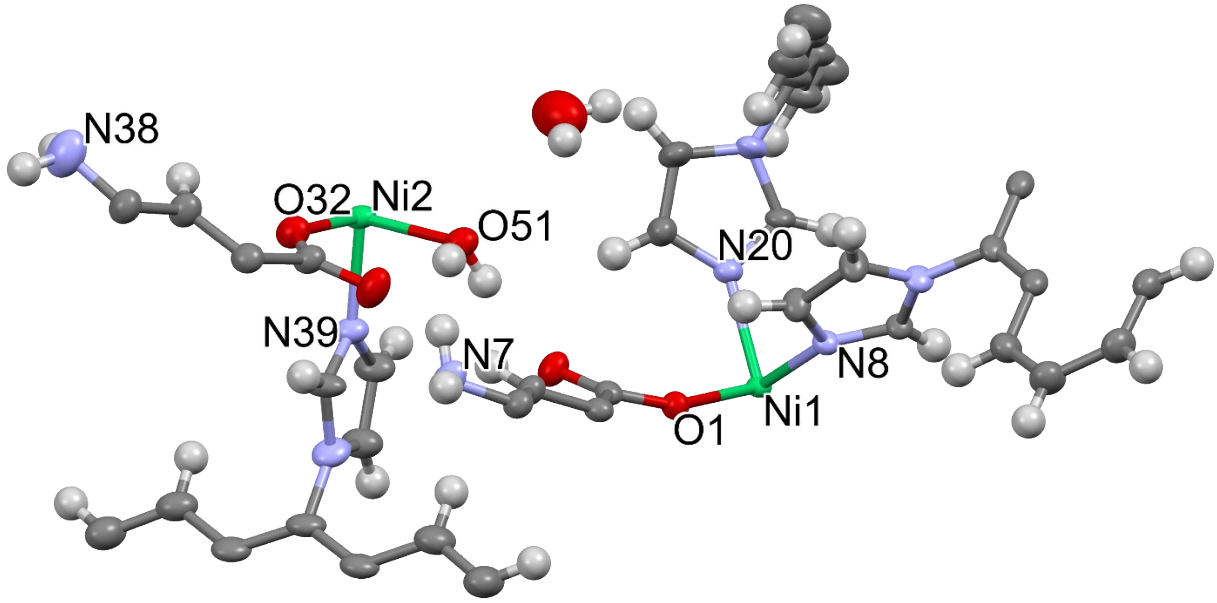

Figure S11. Asymmetric unit of structure **4.** Thermal ellipsoids of atoms are presented at 50 % probability level.

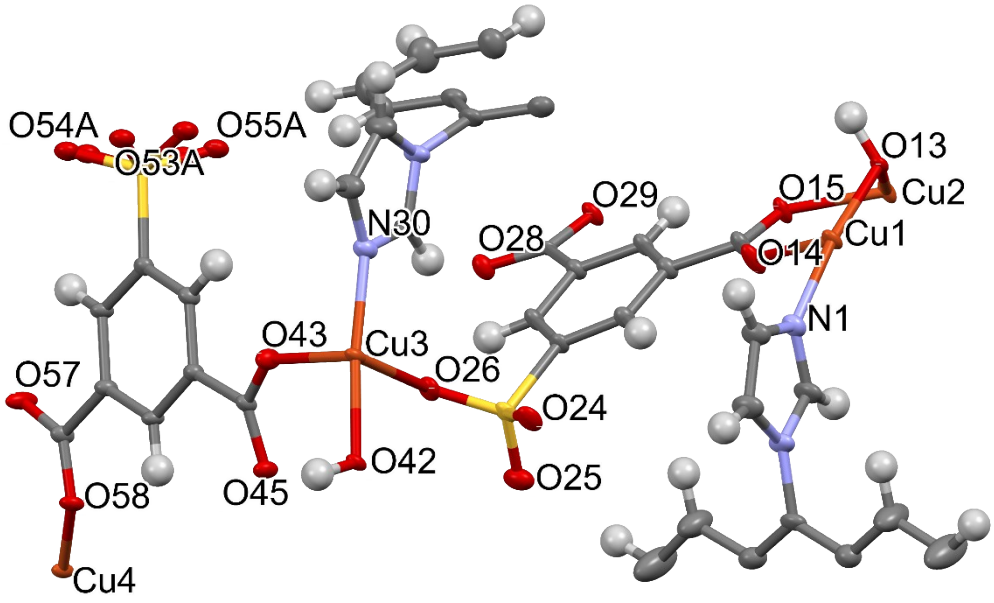

Figure S12. Asymmetric unit of structure **5.** Thermal ellipsoids of atoms are presented at 50 % probability level.

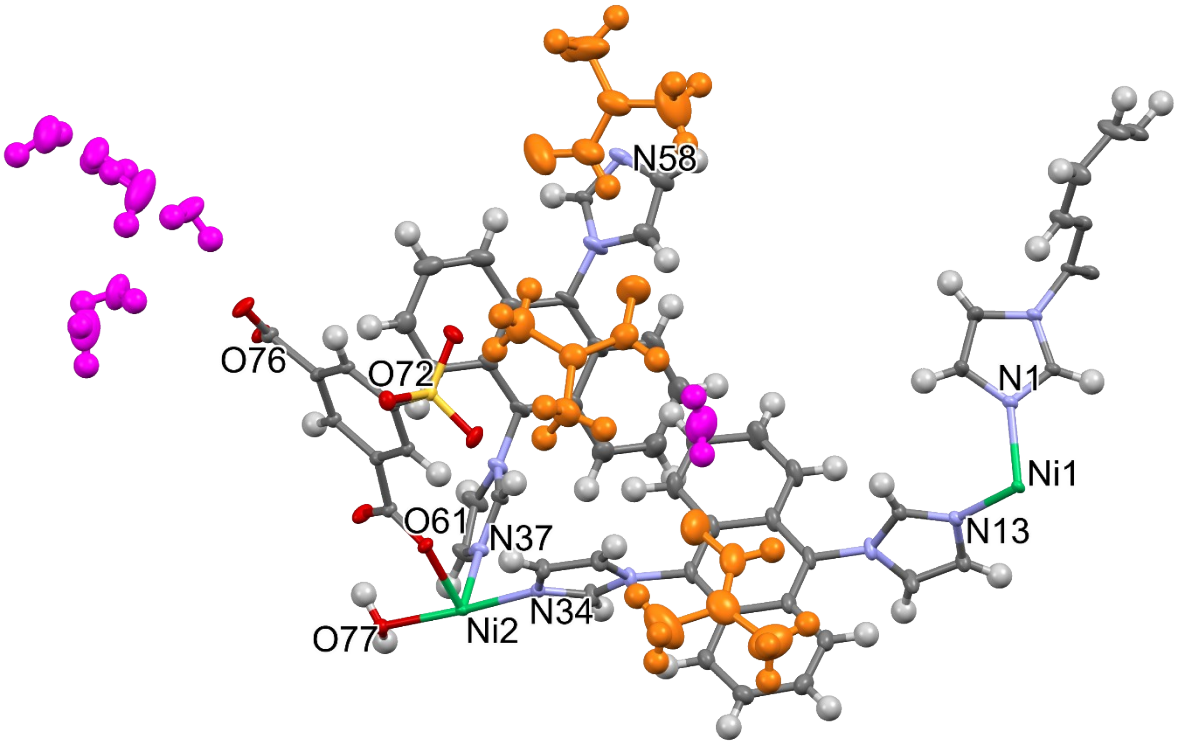

Figure S13. Asymmetric unit of structure **6**. Uncoordinated DMF and water molecules are coloured in orange and purple, respectively. Thermal ellipsoids of atoms are presented at 50 % probability level.

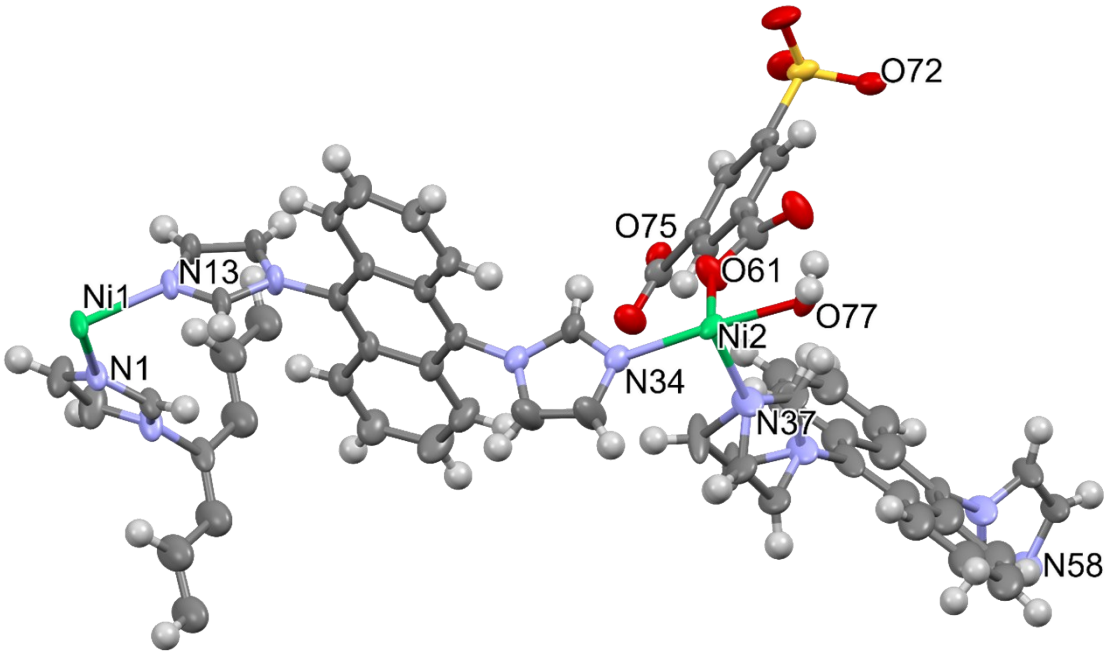

Figure S14. Asymmetric unit of structure **6B (-153 °C).** Uncoordinated solvent molecules removed by Olex2 solvent mask. Thermal ellipsoids of atoms are presented at 50 % probability level.

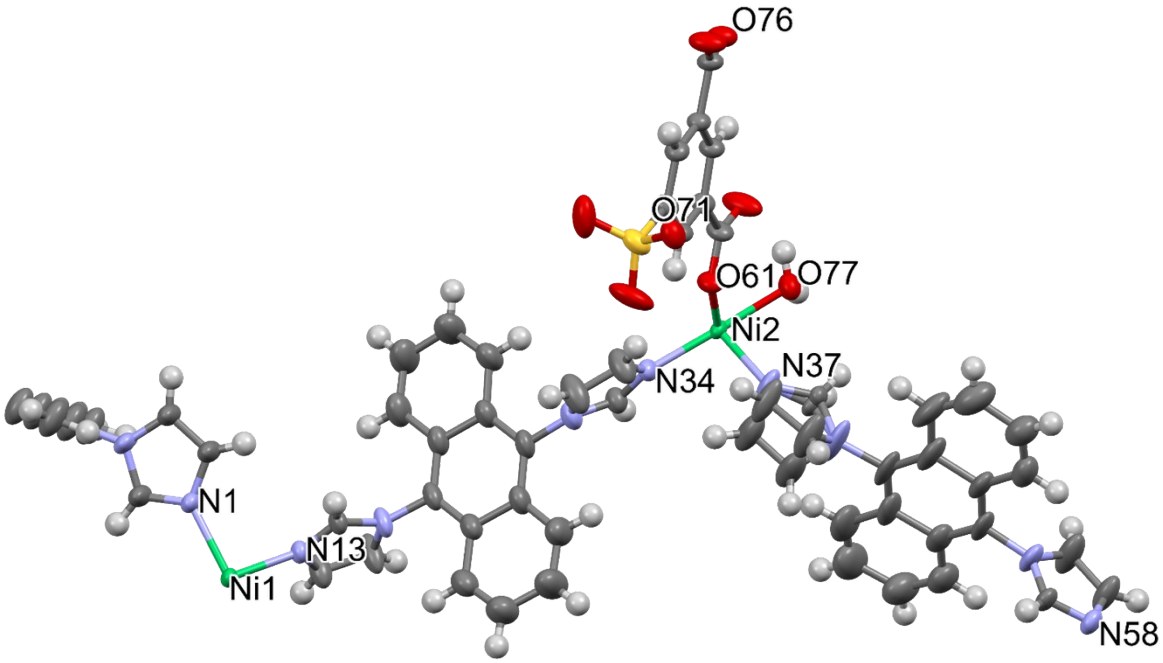

Figure S15. Asymmetric unit of structure **6B (0 °C**). Uncoordinated solvent molecules removed by Olex2 solvent mask. Thermal ellipsoids of atoms are presented at 50 % probability level.

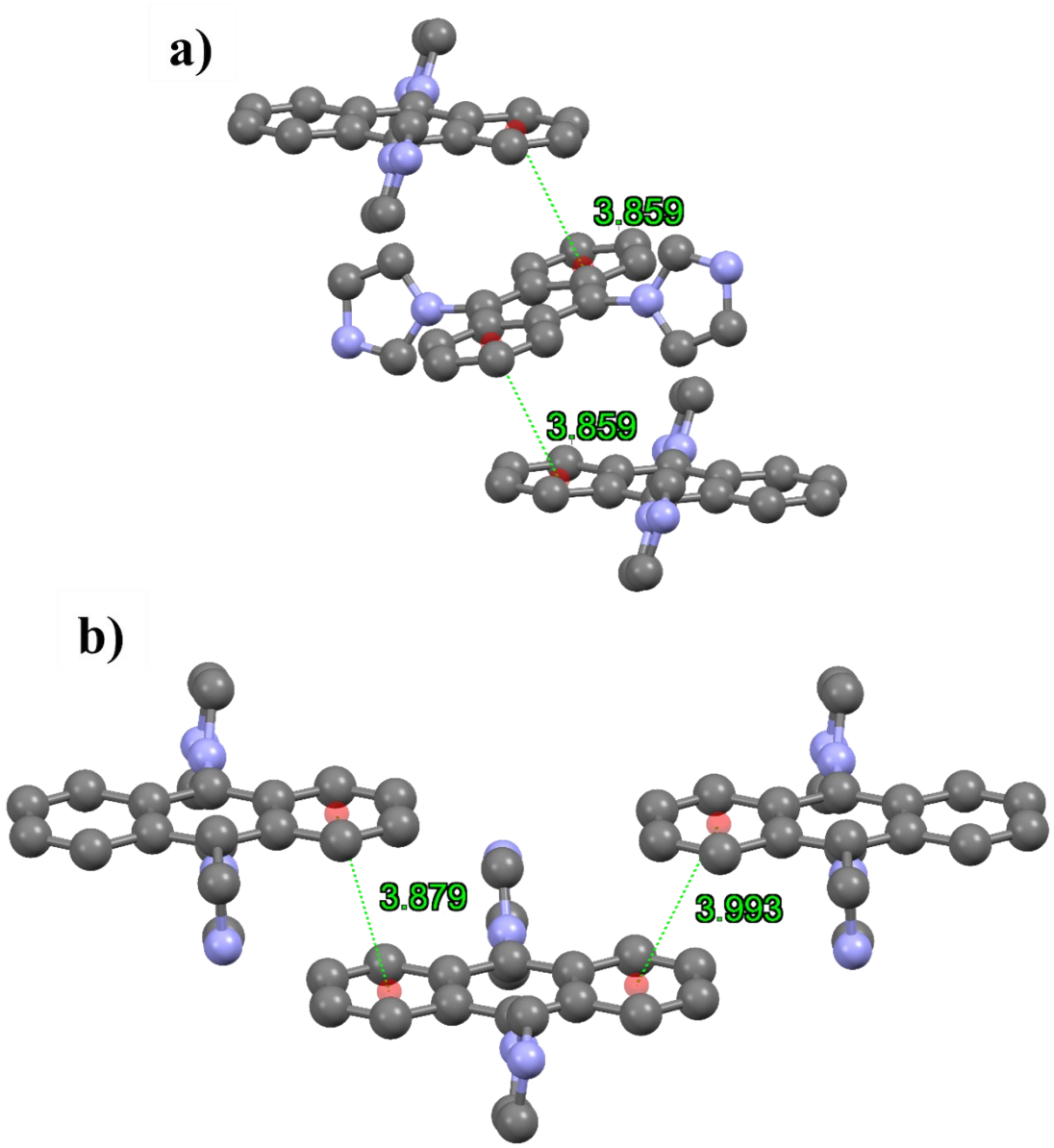

Figure S16. a) π-π interactions between the anthracene rings in structure **1**. b) π-π interactions between the anthracene rings in structure **3**.

PXRD patterns and FT-IR spectra of the synthesized bulk products

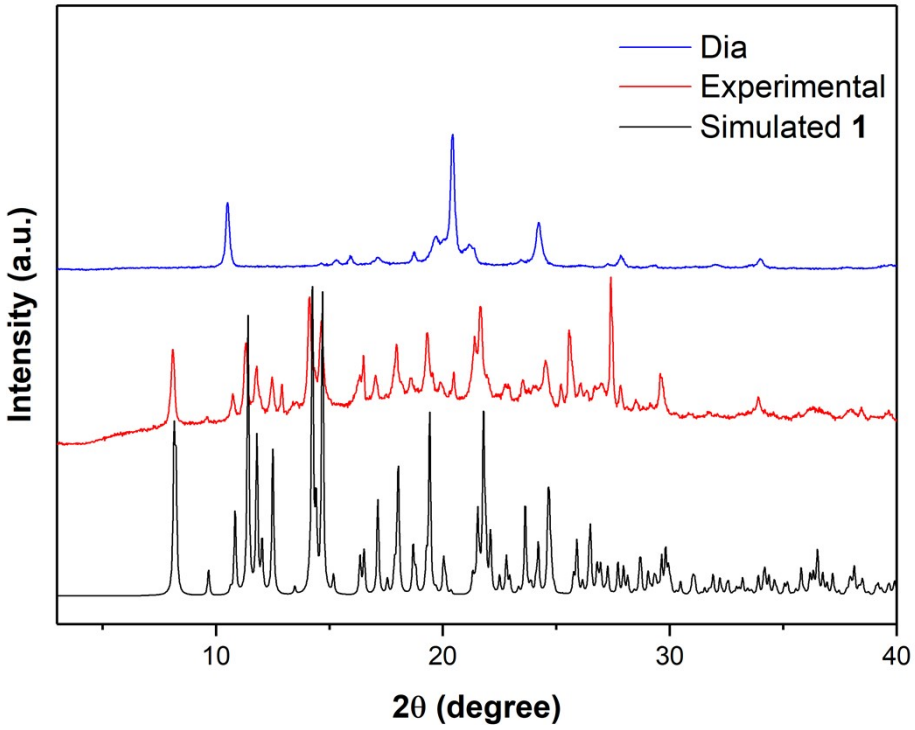

Figure S17. PXRD pattern comparison of neutral dia ligand, impure powder mixture of **1**, and the simulated pattern of **1** from the SCXRD data.

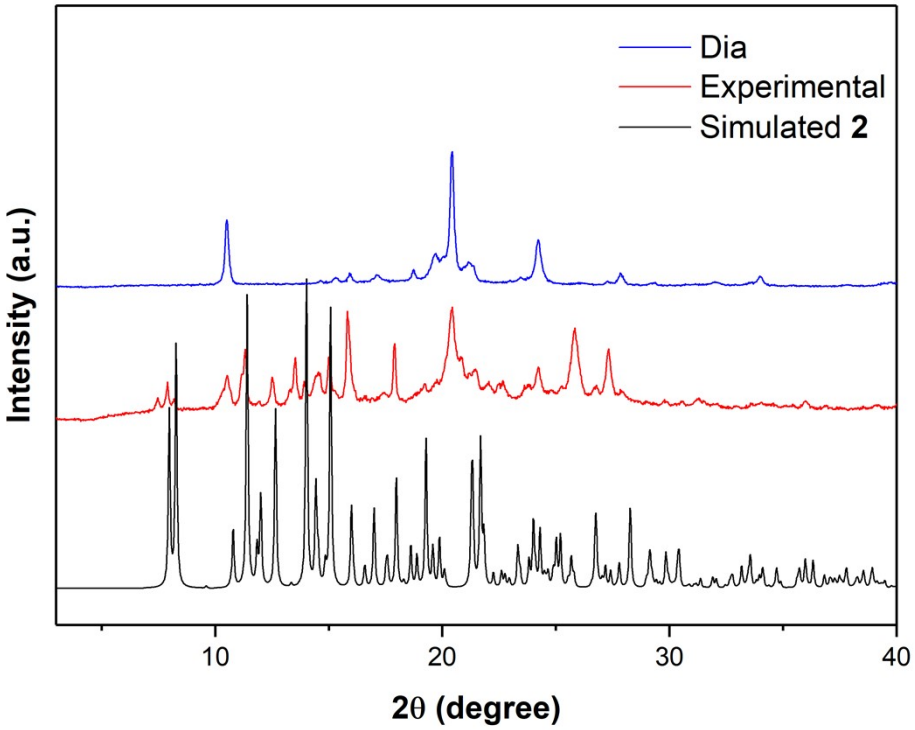

Figure S18. PXRD pattern comparison of neutral dia ligand, impure powder mixture of **2**, and the simulated pattern of **2** from the SCXRD data.

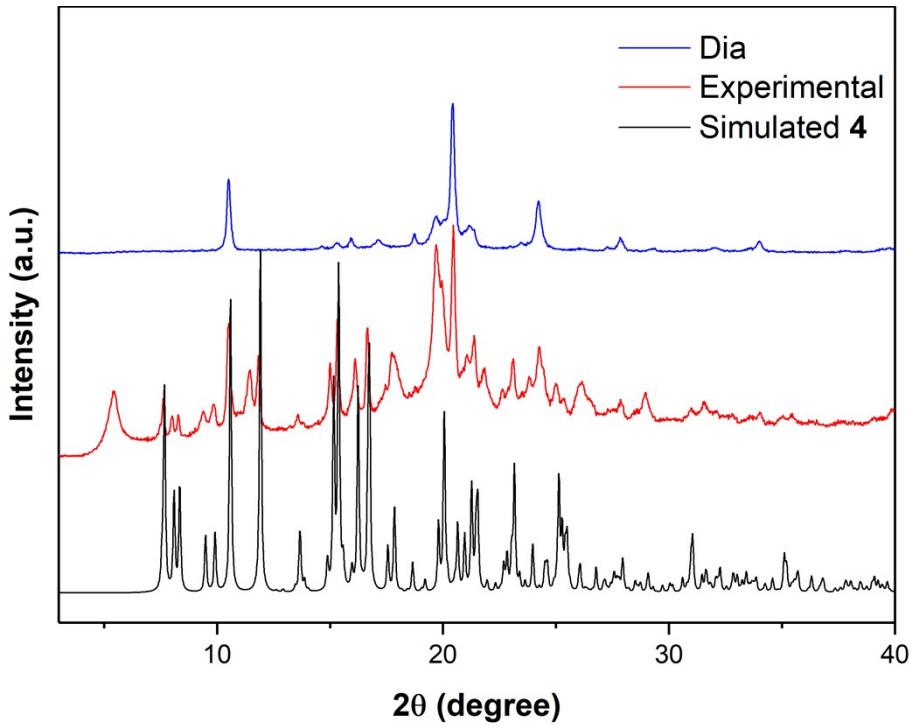

Figure S19. PXRD pattern comparison of neutral dia ligand, impure powder mixture of **4**, and the simulated pattern of **4** from the SCXRD data.

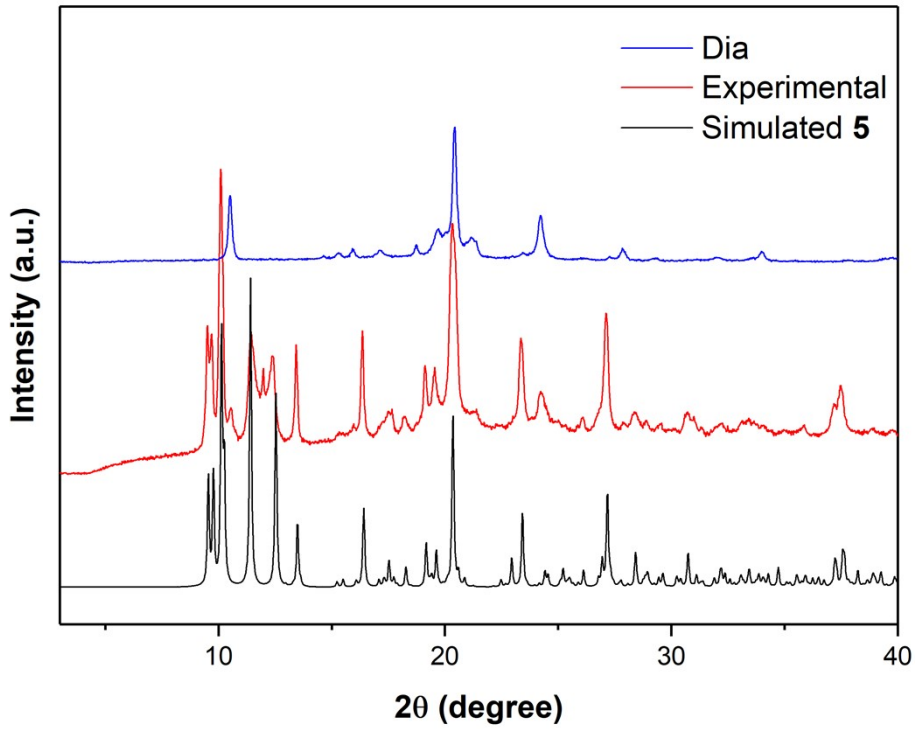

Figure S20. PXRD pattern comparison of neutral dia ligand, impure powder mixture of **5**, and the simulated pattern of **5** from the SCXRD data.

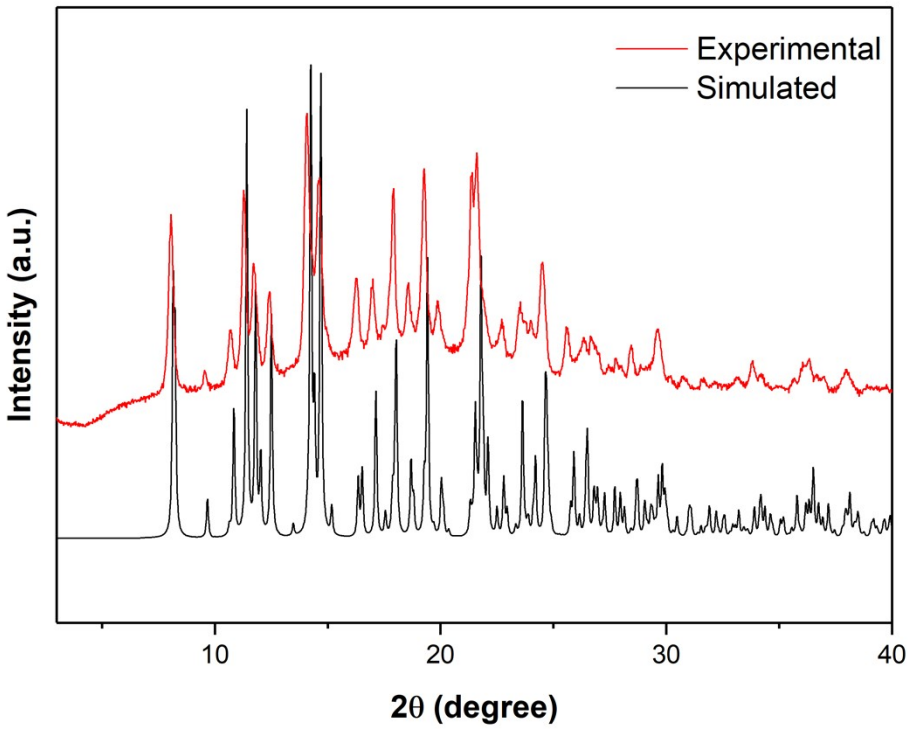

Figure S21. PXRD pattern comparison of the synthesized **1** bulk powder and the simulated pattern from the SCXRD data.

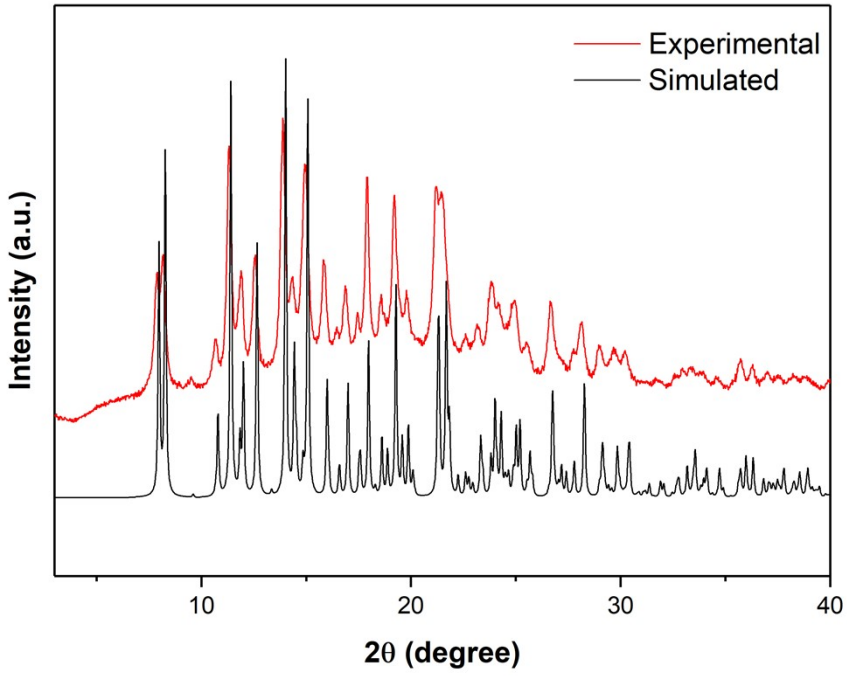

Figure S22. PXRD pattern comparison of the synthesized **2** bulk powder and the simulated pattern from the SCXRD data.

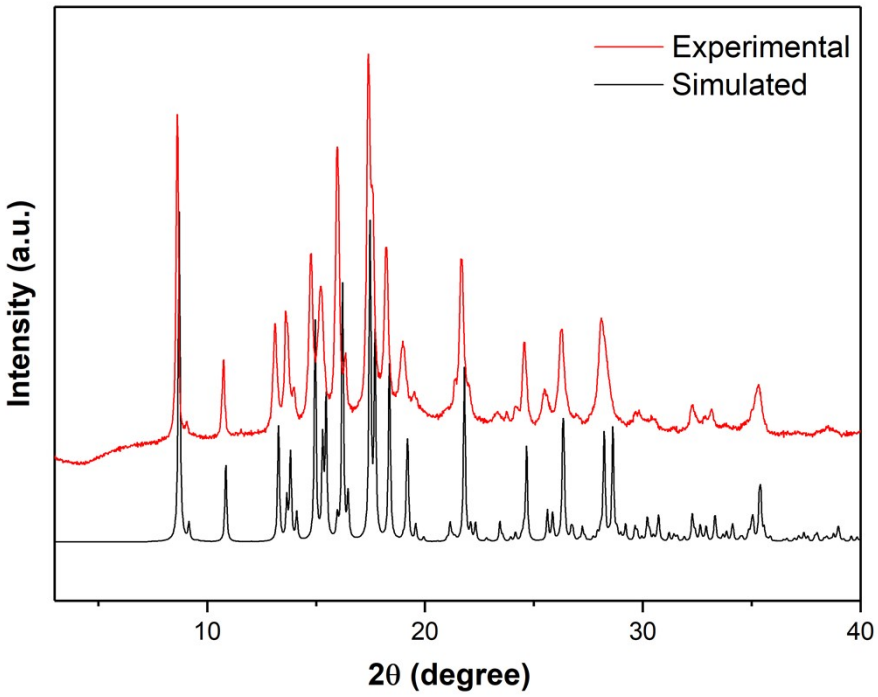

Figure S23. PXRD pattern comparison of the synthesized **3** bulk powder and the simulated pattern from the SCXRD data.

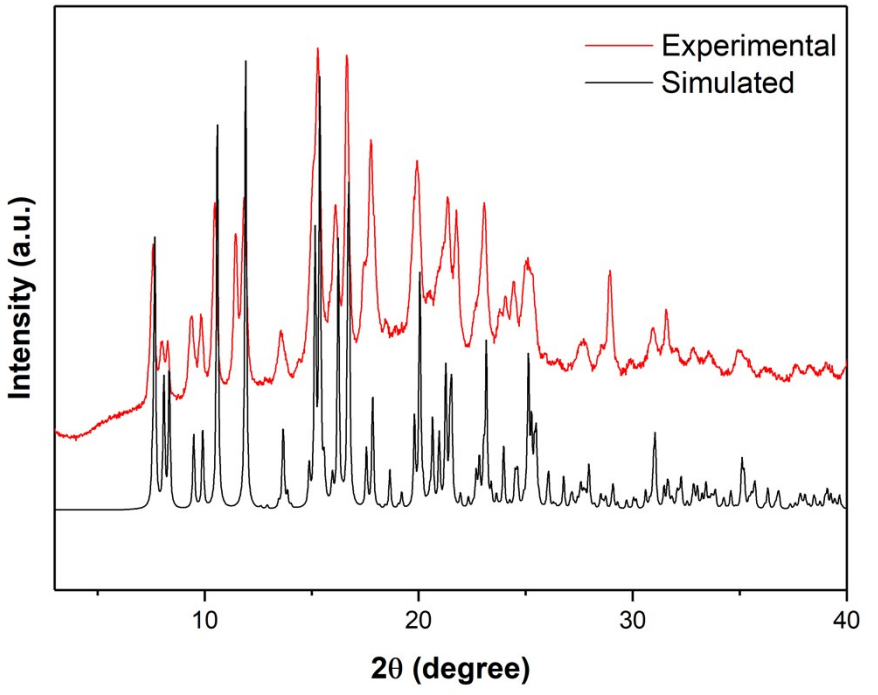

Figure S24. PXRD pattern comparison of the synthesized **4** bulk powder and the simulated pattern from the SCXRD data.

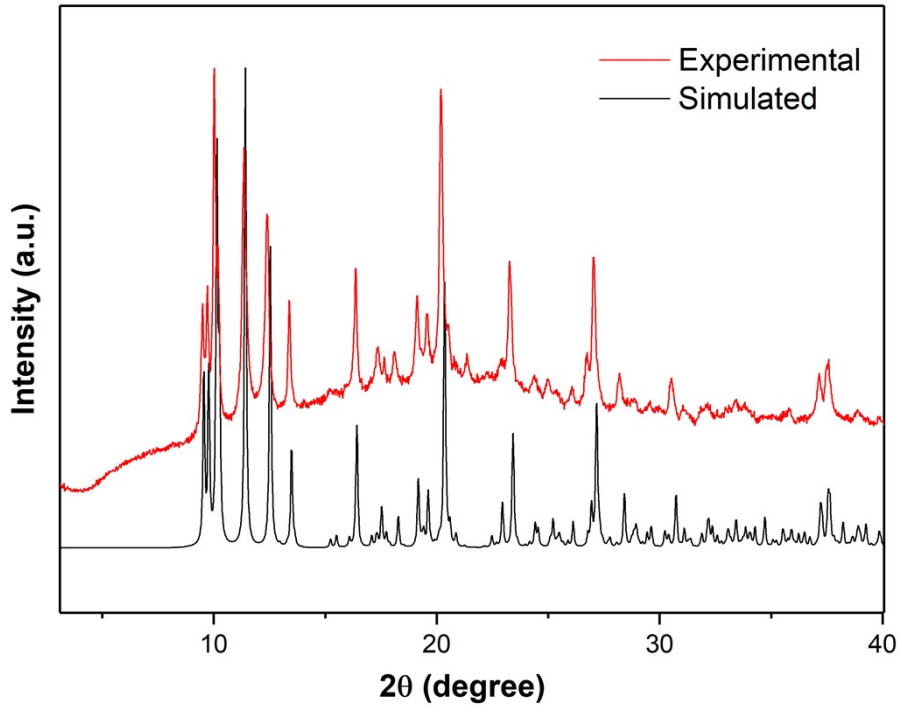

Figure S25. PXRD pattern comparison of the synthesized **5** bulk powder and the simulated pattern from the SCXRD data.

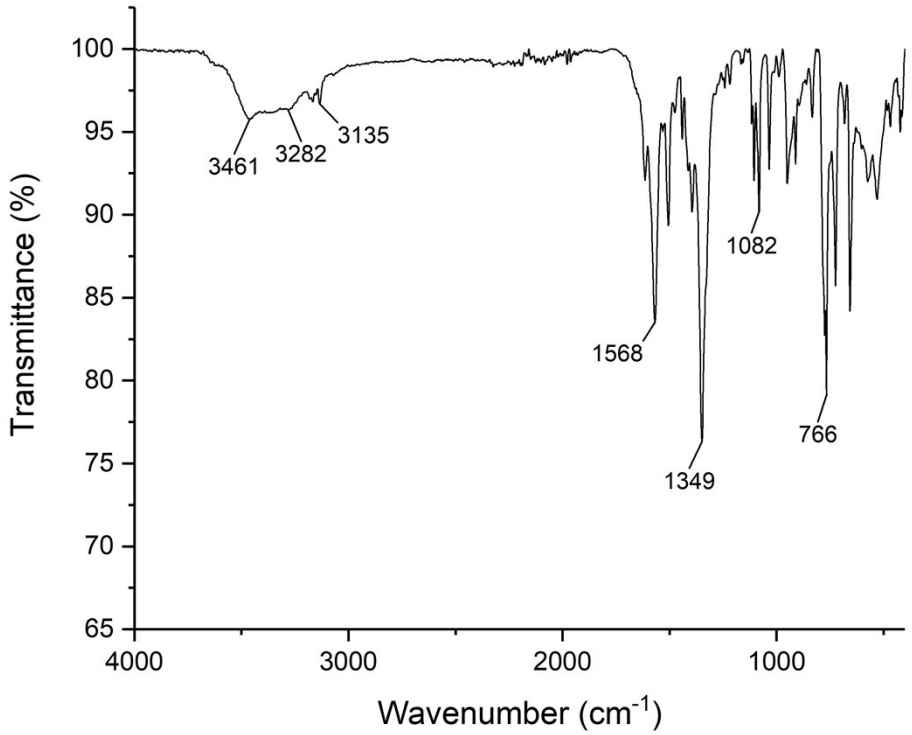

Figure S26. FT-IR spectrum of **1**.

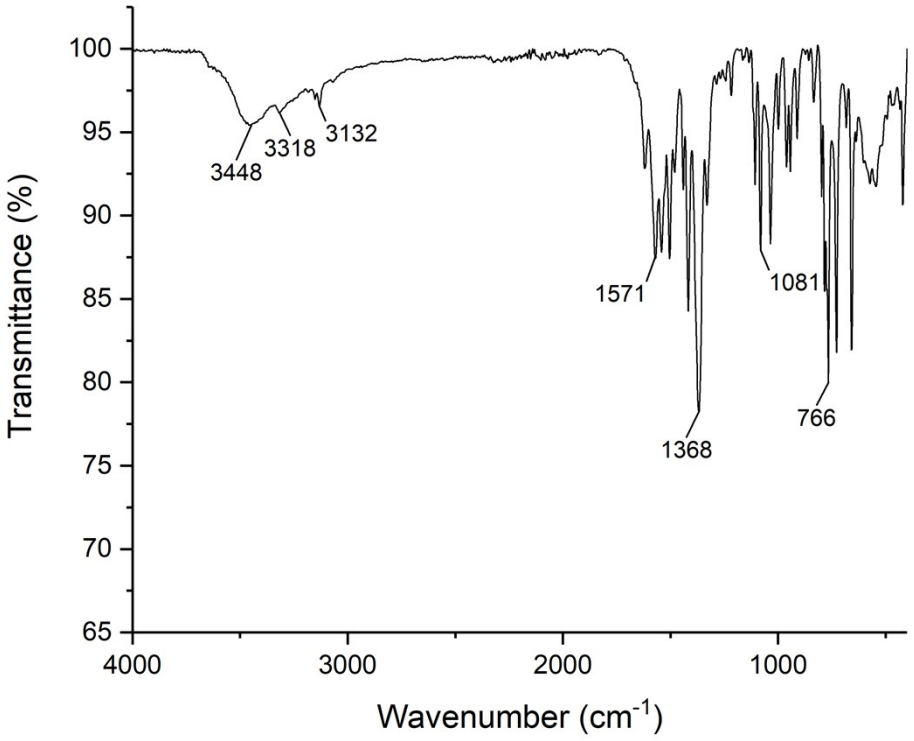

Figure S27. FT-IR spectrum of **2**.

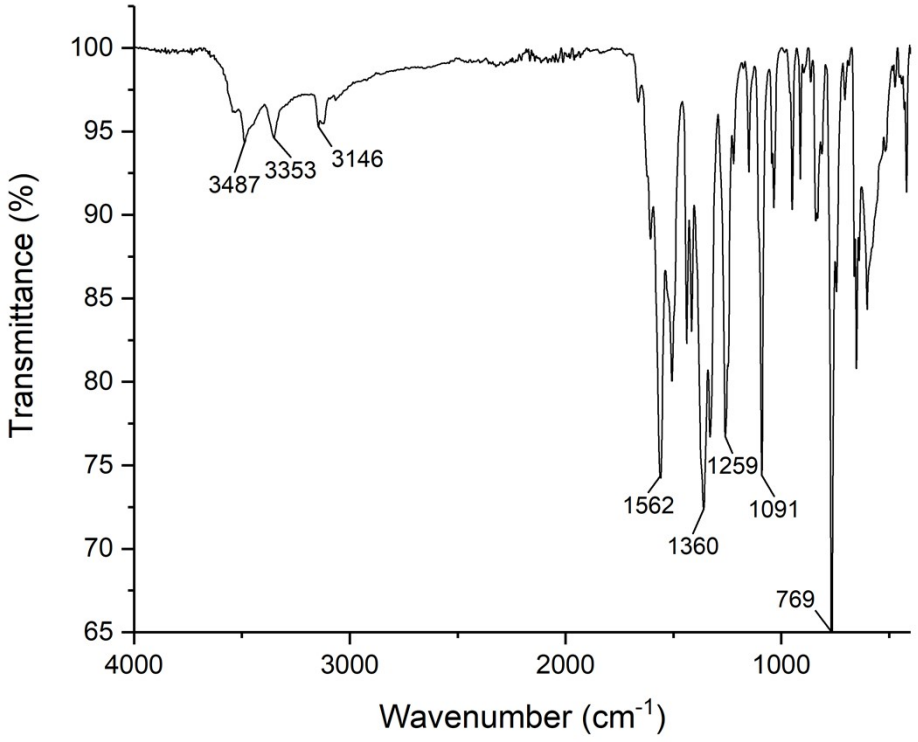

Figure S28. FT-IR spectrum of **3**.

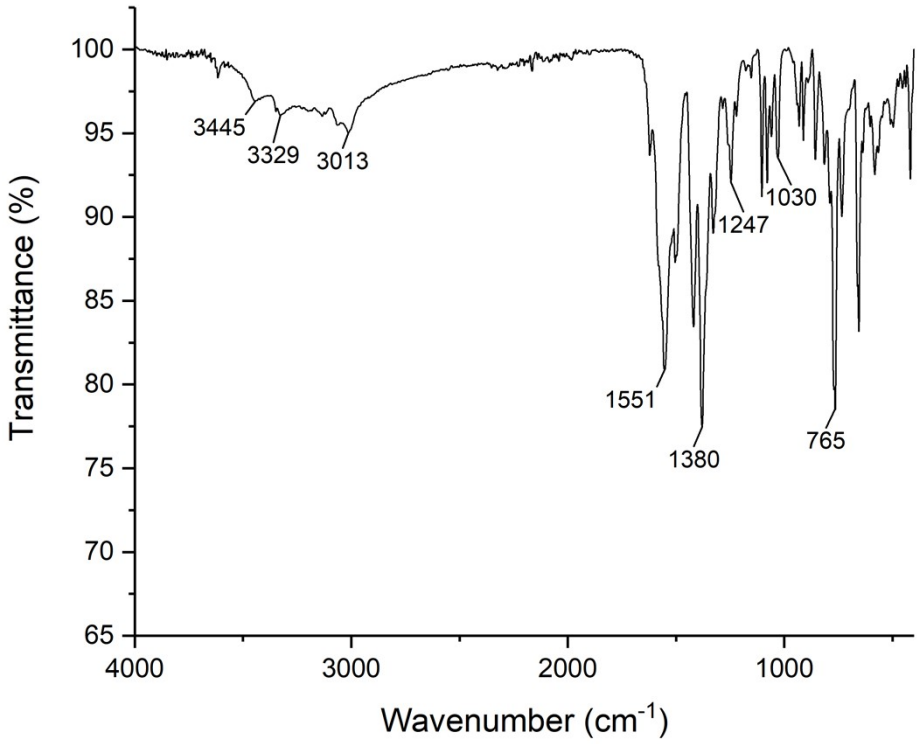

Figure S29. FT-IR spectrum of **4**.

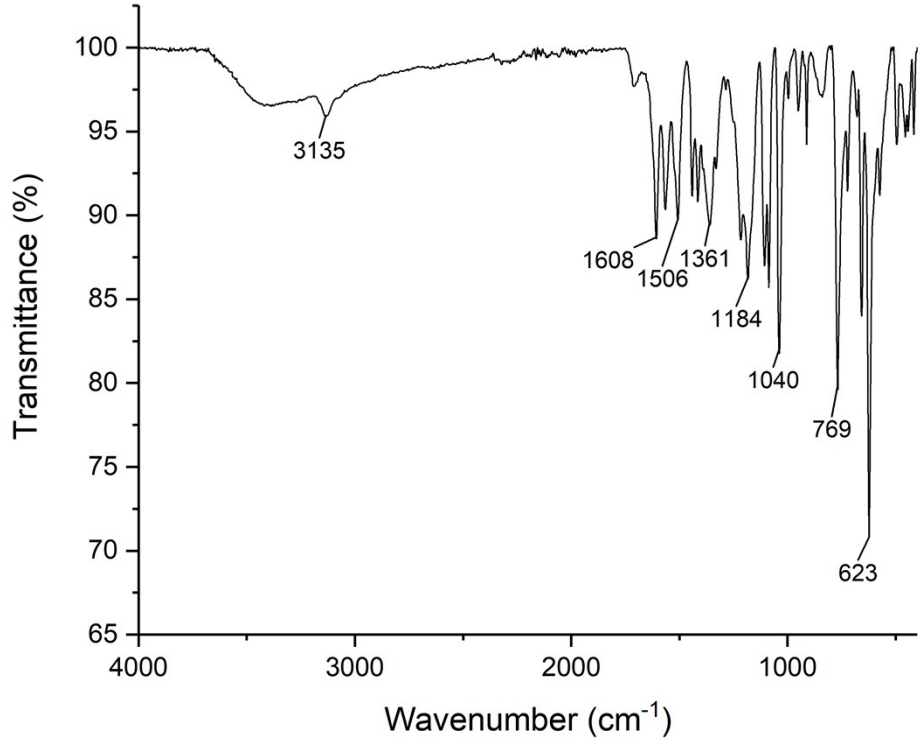

Figure S30. FT-IR spectrum of **5**.

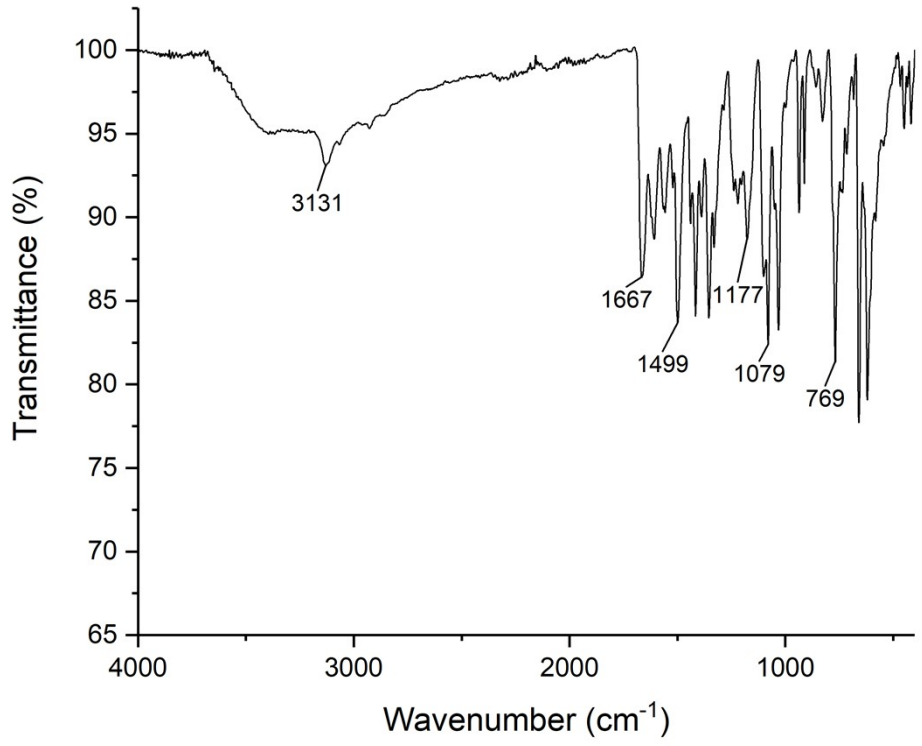

Figure S31. FT-IR spectrum of **6**.

Tauc-plots and optical band gap estimates of the synthesized compounds

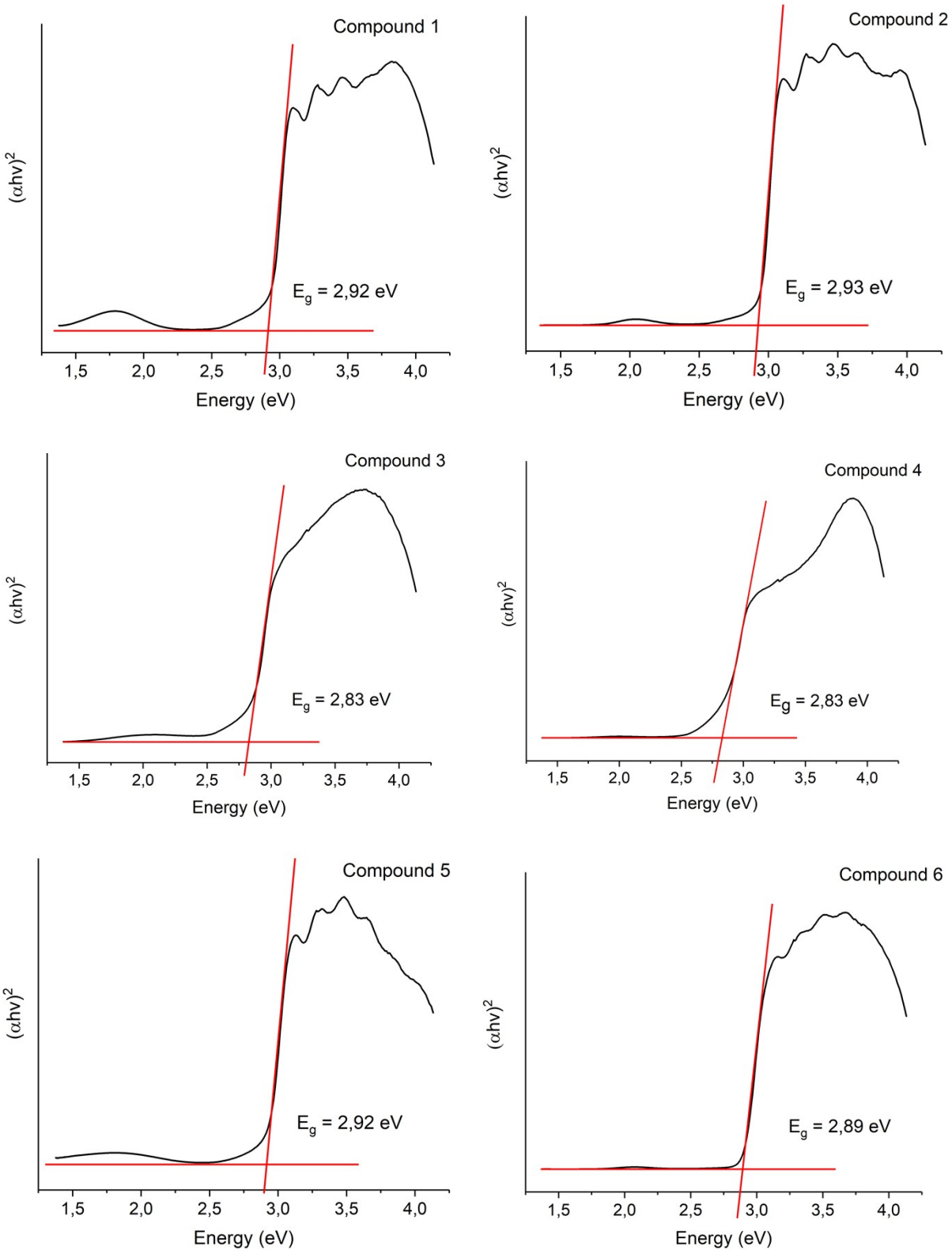

Figure S32. Tauc-plots of compounds **1-6** and their estimated optical band gap values. α = absorption coefficient, h = Planck constant, v = light frequency and E_g = optical band gap.